Compound prism design principles, I

Nathan Hagen[1,2] and Tomasz S. Tkaczyk[1,3]

[1]Department of Bioengineering, Rice University, Houston, Texas 77005, USA

[2]e-mail: nhagen@optics.arizona.edu

[3]e-mail: ttkaczyk@rice.edu

Received 26 May 2011; accepted 5 July 2011;
posted 12 July 2011 (Doc. ID 148098); published 30 August 2011

Prisms have been needlessly neglected as components used in modern optical design. In optical throughput, stray light, flexibility, and in their ability to be used in direct-view geometry, they excel over gratings. Here we show that even their well-known weak dispersion relative to gratings has been overrated by designing doublet and double Amici direct-vision compound prisms that have 14° and 23° of dispersion across the visible spectrum, equivalent to 800 and 1300 lines/mm gratings. By taking advantage of the multiple degrees of freedom available in a compound prism design, we also show prisms whose angular dispersion shows improved linearity in wavelength. In order to achieve these designs, we exploit the well-behaved nature of prism design space to write customized algorithms that optimize directly in the nonlinear design space. Using these algorithms, we showcase a number of prism designs that illustrate a performance and flexibility that goes beyond what has often been considered possible with prisms. © 2011 Optical Society of America

OCIS codes: 230.5480, 080.2740, 260.2030, 300.6190.

1. Introduction

Prisms are commonly used components of spectrometers, and are often preferred over gratings when the desired dispersion is weak. In this regime, they possess better throughput than their grating counterparts, better stray light characteristics, are easier to configure into a direct view geometry (in which the central wavelength passes through the system with its angle unchanged), and are more customizable. We concentrate below on these last two characteristics, and argue that prisms have been unnecessarily neglected in modern spectrometry. With compound prisms, the optical designer has excellent flexibility, enabled by choosing the angles of the prism elements, the glasses that comprise them, and adding additional elements into the design for optimal performance.

The ability to configure prisms for direct view geometry is an advantage that many researchers have used in their instruments, and which was first realized by Amici in 1865 [1]. However, despite their importance for spectrometer design, the principles of designing these direct view, or "nondeviating," prisms is not only scattered across a number of journal papers spanning 150 years, it is also incomplete. Because of the scattered state of the historical literature, it can be difficult to give proper credit to prior work, and so we start with a survey of past work on direct-vision prisms going back to Amici's initial invention. Using the modern sign convention, we present the nonlinear prism design equation and its linear counterpart derived from the small-angle approximation. Regarding compound dispersive prisms, the existing literature has focused exclusively on the latter, but we show that it is easy to work directly with the nonlinear equation for prism dispersion. This provides for a rapid means of optimizing over all available glasses, and for customizing a design for any given system requirements.

We next introduce the concept of dispersion linearity and show that one can improve the linearity of the spectrum by brute force optimization across all glass combinations within a glass catalog. Because the design space is not of high dimension and is relatively

0003-6935/11/254998-14$15.00/0

well behaved, nonlinear optimization algorithms can rapidly obtain solutions, making such a large search practical. This is the first discussion, to our knowledge, of an end-to-end design for dispersion linearization. We find that while an optimization over glass choice can substantially improve linearity, highly linear dispersion from prisms using only two elements can only be achieved within short spectral ranges. Three-element compound prisms such as the double Amici design can achieve substantially linear-in-wavelength dispersion, but we show that there is always a trade-off in prism size.

A surprising result obtained with our design algorithms is that, despite the weak dispersion allowed by two-element direct-vision prism geometry, we show that it is possible to achieve $>14°$ of dispersion across the visible spectrum in a two-element direct-vision design. In a double Amici design, we show that it is possible to achieve 23° of dispersion across the visible spectrum, while maintaining direct-vision geometry. The entire source code (written in Python) used for the designs and all algorithms used to produce the results in this paper can be found on the authors' website [2].

2. Historical Survey of Direct-Vision Dispersive Prism Design

The historical literature on nondeviating prisms invariably miscites the original references, perhaps due to their obscurity. But the recent opening up of old documents to direct electronic access allows one to trace developments, beginning with Amici's initial invention. Amici himself never published about his nondeviating prism, but rather communicated the idea to his friend Donati, who was able to construct the device and use it for observations of stellar spectra. These were published in 1862 [1,3] (an abstract in English was also published in 1863, but mentions only Donati's observations on stellar spectral lines and not Amici's prism [4]). Ref. [1] is almost universally given with the wrong author—Amici instead of Donati—and the incorrect publication date of 1860, though the manuscript itself is signed by Donati with a date of 1860.

Upon hearing of Amici's idea, the French astronomer P. J. C. Janssen (often referred to in the historical literature as Jules Janssen) contributed a paper describing three modifications of the concept [5]. The first describes splitting the double Amici prism in two at the plane of symmetry, allowing one to manipulate the two sides independently. The second modification takes advantage of this splitting to silver the second element, so that the prism is used in reflective Littrow geometry. The third design constructs a compound prism based on Amici's principle but composed of five elements instead of three in order to produce greater dispersion [6]. The first manuscript to show illustrations of Amici's and Janssen's direct-view prisms is apparently Secchi's treatise on the stars [7].

In what was apparently an independent invention, in 1864, Browning in England came up with a three-element prism designed not for zero deviation but rather for reduced deviation. This triplet setup used two thin prisms of crown glass placed on both sides of a single liquid prism of carbon disulfide, and was intended to increase the number of prisms that could be admitted in a circular arrangement common at the time for increasing spectral dispersion. The entire setup was manufactured on the instruction of Gassiot, and consisted of 11 prisms in all [8]. (The invention is also discussed by Browning himself in Ref. [9].)

In 1865, the English astronomer Hershel described a method for constructing single-element direct-vision prisms based on the use of internal reflections [10]. (An illustration of the prism appears in [11]). This design, however, seems to have been used only rarely, possibly due to the low value of dispersion obtained. Emsmann also describes a single-element direct-vision approach [12], and Fuchs later showed how to achieve the same nondeviation effect using a plane mirror external to the prism [13]. Liveing and Dewar continued along these lines and developed a new nondeviating prism design using three air-spaced prisms and two reflecting surfaces [14]. (See Ref. [15] for a modern paper that independently developed this approach and gives alternative geometries.)

Tait (1872) mentions the construction of a three-element nondeviating prism in which all three elements are composed of different materials—a generalization of the double Amici in which the outer elements are composed of the same material [16]. This is a subject we explore in Papers II and III of this series [17,18].

Thollon, in 1878, was apparently the first to give explicit expressions for the design of double Amici prisms, though this work was quickly followed by the more detailed paper of Riccó [19–21]. Thollon also goes on to show that one can reduce the angles of the outer crown prism elements, and increase the angle of the inner flint prism, in order to increase the dispersion of the system as a whole [22].

In 1881, Zenger noted that a design need not use prism materials whose refractive indices are substantially different [23]. Rather, one can construct a nondeviating prism in which the ray for the central wavelength is entirely unrefracted: the prism elements have the same mean refractive index, and the exterior faces of the prism are orthogonal to the optical axis. Only the dispersion is different between the three glass elements. This produces a weak dispersion, so that Wernicke proposed converting the two-element Zenger design into a double Amici configuration—a system in which the mean indices of all three elements are equal [24]. Tyrrell and Conn provide a detailed analysis of this Wernicke-type prism design [25], and also point out that the liquid prisms are not much used because of the strong temperature

dependence in the refractive index of optical liquids, which makes calibration difficult.

Abbott and Fowle (1900) are the first researchers of which we are aware that explicitly attempt to linearize a compound prism's dispersion, and they also aim at doing this for a direct-vision system [26]. They mention using a double Amici prism design composed of a central 20° prism element of rock salt between two elements of 5° 10 arc min flint glass, but present only dispersion measurements for a two-element system, illustrating the improvement in linearity empirically. More recently, the same goal of a linearized nondeviating prism was attempted by Ebizuka *et al.*, using a three-element prism of three different glasses [27]. Blechinger *et al.* show several linearized prism designs for deviating prisms [28], and Bittner *et al.* develop an Offner-type imaging spectrometer using one or more Féry prisms cemented together, showing that one can linearize the dispersion by proper selection of the glasses and angles [29]. Refs. [26–29], however, only briefly mention design issues, and do not give quantitative design methods. One is left with the impression that these authors constructed their designs using trial and error, aided by optical design software.

E. and T. Dereniak, on the other hand, take advantage of theory developed for superachromat lenses [30,31] to give explicit expressions for the first-order design of compound nondeviating prisms with linearized dispersion ([32]), allowing one to see the explicit dependence on the mean index, Abbe V-number, and partial dispersion of the glasses used in the design. (See Section 4 below, and also Section 2 of Paper II [17].) An early book that appears to contain relevant material, but which has proven inaccessible to us, is Ref. [33].

A clever adaptation of the double Amici was developed by Wynne for atmospheric dispersion correction [34]. This takes advantage of the plane of symmetry in the center of a double Amici system, allowing for the physical separation of the two sides of the prism (as in Ref. [5]). By rotating both sides in equal and opposite azimuth angles, one has a nondeviating disperser with tunable dispersion.

Our own interest in the subject of nondeviating prisms stems from their use in imaging spectrometers [35,36] and from our own research group's need to develop better performing designs.

3. Simple Prisms: First-Order Design Principles

The refraction of a ray through a simple prism (Fig. 1) is given by applying Snell's law at each interface such that

$$\left.\begin{aligned} \theta_1 &= \theta_0 - \beta, & \theta_2' &= \arcsin(n\sin\theta_2),\\ \theta_1' &= \arcsin\left(\tfrac{1}{n}\sin\theta_1\right), & \theta_3 &= \theta_2' + \gamma,\\ \theta_2 &= \theta_1' - \alpha, \end{aligned}\right\}, \quad (1)$$

where we assume that the optical axis is parallel to the prism base, the external medium has refractive

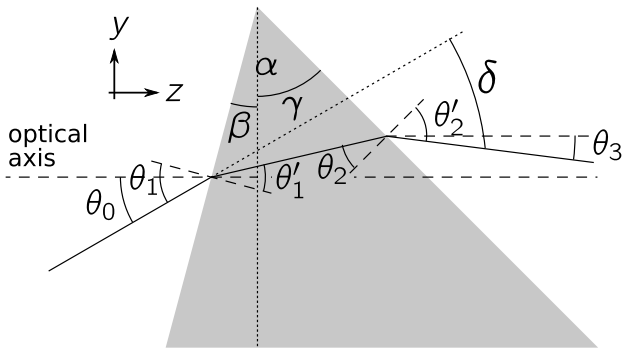

Fig. 1. Ray trace through a simple prism. The ray is incident at an angle θ_0 from the optical axis (dashed); θ_1, θ_1', θ_2, and θ_2' are the angles of incidence and refraction on the first and second prism interfaces, and θ_3 is the angle of the deviated ray with respect to the axis. The prism shown here has an apex angle $\alpha = 60°$ and is oriented such that the front and back faces of the prism have angles $\beta = -15°$ and $\gamma = 45°$ with respect to the optical axis. The prism has an index of refraction $n = 1.5$, a height h, and an axial thickness t. For the ray traced here, $\theta_0 = 30°$ and $\theta_3 = -7.4°$, such that $\delta = 37.4°$. Using the sign convention, θ_1 and θ_1' are positive quantities, while θ_2 and θ_2' are negative. The quantity Δy is the beam displacement.

index 1, $\alpha = \gamma - \beta$, and the angles are defined as shown in Fig. 1. The angles θ_i follow the modern sign convention [37], in which clockwise angles traced from the surface normal to the ray have *negative* sign, and counterclockwise angles have *positive* sign. The deviation angle δ is simply

$$\delta = \theta_0 - \theta_3 = \theta_1 - \theta_2' - \alpha.$$

Since the prism refractive indices vary with wavelength, so too does the deviation angle. The difference in deviation angle between the two extreme wavelengths transmitted by the prism is the dispersion Δ:

$$\Delta = \delta(\lambda_{\min}) - \delta(\lambda_{\max}) \equiv \delta_{\max} - \delta_{\min}.$$

In classical optical design, this is commonly written as $\Delta = \delta_F - \delta_C$ for the Fraunhofer F and C wavelengths ($\lambda_F = 486\,\text{cm}$, $\lambda_C = 656\,\text{cm}$). We use $\bar{\lambda}$ for the central wavelength, defined as $\bar{\lambda} = \frac{1}{2}(\lambda_{\max} + \lambda_{\min})$, rather than the conventional λ_d (note that the central wavelength and the mean wavelength can be different when the dispersion is sampled nonuniformly, as is typically the case in prism spectra). The spectral dispersion is thus a function of the glass dispersion $n(\lambda)$, the prism apex angle α, and the incident ray angle θ_0.

The refraction Eqs. (1) represent the nonlinear relationship of dispersion $\delta(n(\lambda), \alpha, \theta_0)$ to each of the system variables. In order to obtain an estimate of the appropriate design variables from the desired dispersion, the historical approach has been to assume small prism angles α and small angles of incidence θ_0. Using these approximations reduces the exact form obtained by combining the refraction equations,

$$\delta = \theta_0 - \gamma - \arcsin\left(n \sin\left(\arcsin\left(\frac{1}{n}\sin(\theta_0 - \beta)\right) - \alpha\right)\right),$$

to the simple linear form

$$\delta = (n-1)\alpha, \tag{2}$$

from which the prism apex angle α is trivially obtained from the desired dispersion and the glass refractive index. A *nondeviating* prism is defined as a disperser in which the deviation of the central wavelength is zero: $\delta(\bar{\lambda}) = 0$. This can be achieved with the addition of a second prism element.

Other useful quantities to know about a prism are the minimum prism height $h_{\min}$, the minimum axial thickness $t_{\min}$, minimum displacement $\Delta y_{\min}$, and the exit beam width w' for a given incident beam width w. These are readily calculated from geometry as

$$\begin{aligned} t_{\min} &= h_0(\tan\gamma - \tan\beta), \\ \Delta y_{\min} &= h_0 \frac{\sin(\alpha)\sin(\theta_1' + \beta)}{\cos(\beta)\cos(\theta_2)}, \\ h_{\min} &= \max\{h_0, h_0 + \Delta y\}, \\ w' &= w\cos(\theta_2')/\cos(\theta_1), \end{aligned}$$

where $h_0 = w\cos(\beta)/\cos(\theta_1)$, and they are illustrated in Fig. 2.

4. Two-Element Prisms: Linear and Nonlinear Design Approaches

A number of researchers [38–42] have constructed direct-vision compound prisms with two elements ("doublets") using linear design equations. With the small-angle approximations, one can use linear equations to design doublet prisms (as in Fig. 3) having both zero deviation and the desired dispersion [32]. Using the linearity property of these equations, the deviation of the compound element is simply the sum of the individual element deviations,

$$\delta(\lambda) = \delta_1(\lambda) + \delta_2(\lambda) = (n_1(\lambda) - 1)\alpha_1 + (n_2(\lambda) - 1)\alpha_2, \tag{3}$$

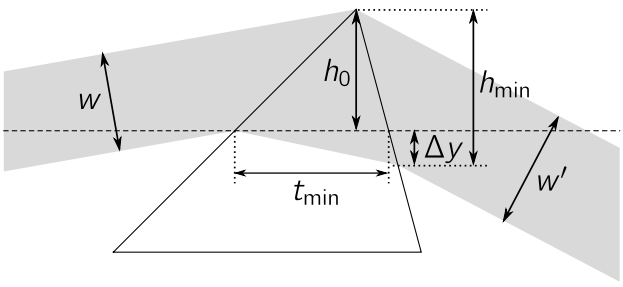

Fig. 2. Incident beam width w is transformed into an exiting beam width w'. The minimum prism height $h_{\min}$ and minimum prism axial thickness $t_{\min}$ are constrained by the beam width, prism geometry and angle of incidence.

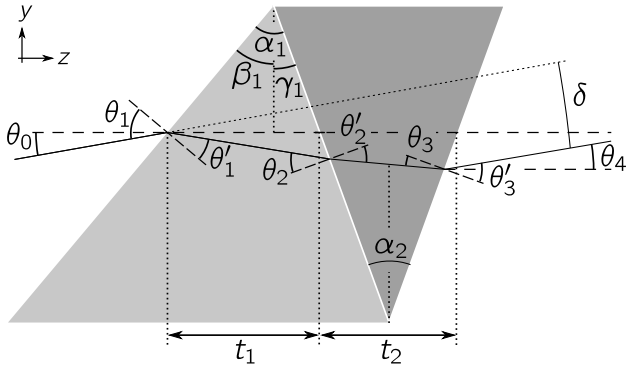

Fig. 3. A ray trace through a doublet compound prism, where the second element is assumed to be oriented symmetrically with respect to the normal to the optical axis. The system shown here has prism apex angles $\alpha_1 = 60°$ and $\alpha_2 = -40°$, indices of refraction $n_1 = 1.5$ and $n_2 = 1.8$, height h, axis-to-apex height h_0, beam displacement Δy, and axial thicknesses t_1 and t_2. The input ray has angle $\theta_0 = 10°$, such that $\delta = 0.4°$.

in which a typical design uses $\alpha_2 < 0$, indicating that the prism is inverted relative to the first prism (as in Fig. 3). If we further assume that the wavelength dependence to the refractive index is approximately linear, then the dispersion can be written as

$$\Delta = \frac{\delta_1(\bar{\lambda})}{V_1} + \frac{\delta_2(\bar{\lambda})}{V_2}, \tag{4}$$

where δ_i and V_i are the dispersion and Abbe number of element i within the compound prism, $V_i = (\bar{n} - 1)/(n_F - n_C)$. If we define the shorthand notation $\bar{\delta} = \delta(\bar{\lambda})$ and let $\bar{\delta} = 0$, solving Eqs. (3) and (4) simultaneously gives

$$\bar{\delta}_1 = -\bar{\delta}_2 = -\Delta\left(\frac{1}{V_2} - \frac{1}{V_1}\right)^{-1}, \tag{5}$$

from which one can obtain the element apex angles α_1 and α_2 from the mean refractive indices of the glasses chosen:

$$\alpha_1 = \frac{\Delta}{\bar{n}_1 - 1}\left(\frac{1}{V_1} - \frac{1}{V_2}\right)^{-1}, \tag{6}$$

$$\alpha_2 = \frac{\Delta}{\bar{n}_2 - 1}\left(\frac{1}{V_2} - \frac{1}{V_1}\right)^{-1}. \tag{7}$$

Most practical prisms do not satisfy the small value approximations closely, so that the typical design procedure is to use the linear Eqs. (3) and (4) to obtain a preliminary solution, after which commercial optical design software is used to perform the final nonlinear optimization. An alternative to the linear design equations is to use the optimization code directly with the nonlinear equation

$$\delta(n_1(\lambda), n_2(\lambda), \alpha_1, \alpha_2, \theta_0),$$

readily obtained by concatenating the prism doublet's refraction equations,

$$\left.\begin{aligned} \theta_1 &= \theta_0 - \beta_1, & \theta_3 &= \theta_2' - \alpha_2, \\ \theta_1' &= \arcsin\left(\tfrac{1}{n1}\sin\theta_1\right), & \theta_3' &= \arcsin(n_2 \sin\theta_3), \\ \theta_2 &= \theta_1' - \alpha_1, & \theta_4 &= \theta_3' + \tfrac{1}{2}\alpha_2, \\ \theta_2' &= \arcsin\left(\tfrac{n_1}{n_2}\sin\theta_2\right), \end{aligned}\right\}, \tag{8}$$

where $\beta_1 = -\alpha_1 + \frac{1}{2}\alpha_2$, $\delta = \theta_0 - \theta_4$, and $\Delta = \delta(\lambda_{\max}) - \delta(\lambda_{\min})$. (See Fig. 3 for an illustration of these quantities.) The convention, followed in all of our two- and three-element prism designs, is to have the second prism placed such that its plane of symmetry is normal to the optical axis. All other prism elements have their positions defined relative to this second element. Angles β_i and γ_i are defined such that $\alpha_i = \gamma_i - \beta_i$ for prism element i, and β and γ define the angles of the prism's front and rear faces relative to the optical axis normal. (Thus, for our convention, the second element always has $\beta_2 = -\gamma_2$.)

In order to gain more flexibility over the design procedure, we use custom written algorithms incorporating nonlinear optimization code [43]. This allows us to illustrate the design space of each prism and analyze its behavior.

From the two quantities δ and Δ, one can define a merit function M whose optimization code can be used to perform the search for a solution. A common choice for M is the sum of square errors in the variables, which in this case gives

$$M = (\bar{\delta} - \bar{\delta}^*)^2 + (\Delta - \Delta^*)^2,$$

where $\bar{\delta}^*$ and Δ^* are the design target values and $\bar{\delta}$ and Δ are values during a given step of the optimization. Figure 4 illustrates the design space for the ray deviation and the spectral dispersion of a BK7–SF6 doublet operating over the visible spectral range (400–700 nm). For the example chosen, the linear equations provide a design of $(\alpha_1, \alpha_2) = (35°, -22°)$ at the intersection of the $\delta = 0$ and $\Delta = 1°$ lines shown. The nonlinear approach finds the optimum at $(\alpha_1, \alpha_2) = (33°, -31°)$, given by the intersection of the dashed curves shown. In this simple case, the linear equations provide a good starting point for the exact design.

Looking at Fig. 4(a), we can see that the (α_1, α_2) design space for the deviation δ is well behaved, with the linear equations somewhat underestimating the magnitude for α_2 needed to achieve direct-vision ($\bar{\delta} = 0$). Figure 4(b), likewise, shows that the design space for the dispersion ($\Delta = 1°$) is also well behaved, with the linear equations again underestimating the magnitude of α_2 over much of its range. One feature to note, however, is the presence of a maximum between the two 0.400 contour lines at the bottom of the figure. This indicates that a secondary minimum of the dispersion function $\Delta(n_1(\lambda), n_2(\lambda), \alpha_1, \alpha_2, \theta_0)$ is

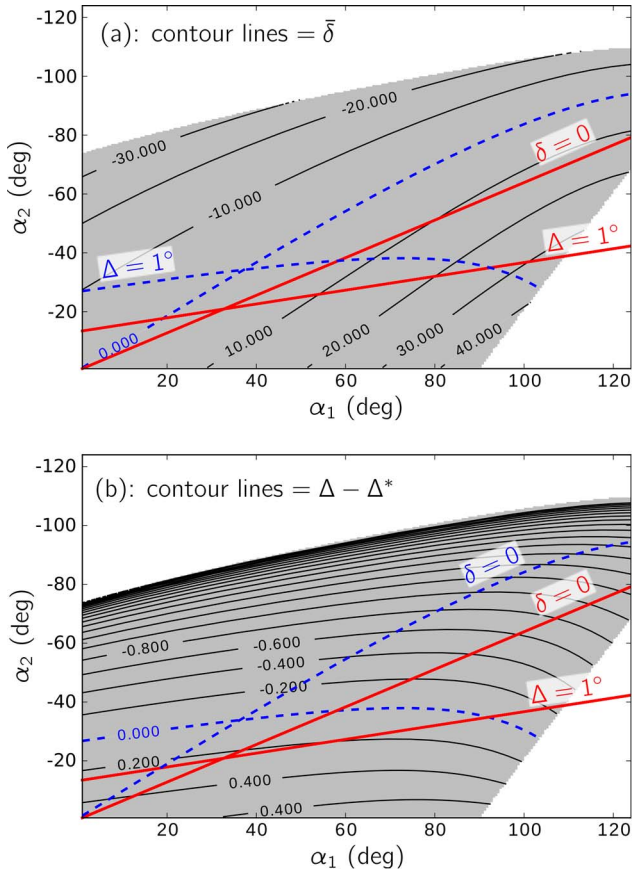

Fig. 4. (Color online) Doublet prism design space, showing contour plots of a, the central deviation $\bar{\delta}(\alpha_1, \alpha_2)$, and b, the difference of the dispersion $\Delta(\alpha_1, \alpha_2)$ from the target value $\Delta^* = 1°$ for a 400–700 nm spectral range and glass choices of BK7 and SF6. The dashed blue lines indicate the (α_1, α_2) values required to meet either the $\bar{\delta}^* = 0$ design target (for direct-vision) or the $\Delta^* = 1°$ target, while the red solid lines indicate prism angles satisfying linear Eq. (5). A design satisfies both targets where the two curves meet, and the gray background indicates the valid design space, outside of which total internal reflections occur at one of the prism interfaces.

forming in the bottom right corner. This feature turns out to be a common one, even in the design space of prisms with three or more elements, and can cause an optimization routine to get stuck inside the secondary minimum. Thus, for doublets we find that it is generally a good idea to overestimate the apex angle of the higher index element (α_2 in this case) when providing a starting guess in doublet designs.

Also, we can observe that since the second element in a doublet compound prism tends to "achromatize" the first (i.e., the dispersions of the two elements tend to cancel rather than to sum constructively), the achievable dispersion is typically weak. Using N-LAK34 and N-SF66 as an example choice of glasses (this glass pair produces a design with small angles α_i), Fig. 5 shows curves for the α_1 and α_2 design points as a function of the dispersion target Δ^* for the visible spectral range (400–700 nm). Beyond about $\Delta^* = 14°$, the angle of incidence θ_1 becomes

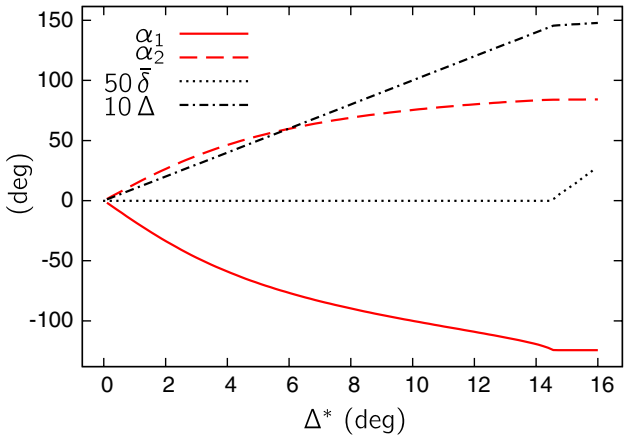

Fig. 5. (Color online) Design parameters of a nondeviating N-LAK34/N-SF66 prism doublet as a function of the target dispersion. The α_1 and α_2 curves proceed in an approximately parabolic curves until about 14.6°, beyond which the system can no longer achieve the target values. In this case, the limit is reached as the front face of the prism approaches the grazing angle to the incident beam (i.e., θ_1 approaches 90°).

extreme, and the design can no longer simultaneously maintain the direct-vision ($\bar{\delta} = 0$) and dispersion targets. This is the design limit for a nondeviating prism doublet using a standard glass set. Considerably larger dispersion than this can be achieved by extending the spectral range, though with a reduced number of glasses available due to absorption effects. (Note that fully depleted silicon detector arrays allow working at high quantum efficiency over a 300–1000 nm range [44,45].)

5. Optimizing over Glass Combination

Unless the types of glasses to be used in the prism are greatly constrained, it is also useful to optimize over available glass types, as it provides additional design flexibility. One can choose a glass pair that not only satisfy the design targets $\bar{\delta}^*$ and Δ^*, but that also, for example, provide the most linear dispersion or the most compact layout among all glass pairs considered. In order to implement glass optimization, we have written code that reads the parameters of all glasses listed in a standard catalog. (This script is made available on the authors' website [2] for all interested readers.) For the greatest accessibility, we have chosen the catalog format provided by the commercial optical design software ZEMAX [46], and performed a brute force search over all glass combinations within the full set or any subset of catalogs. The results of all glass combinations that can satisfy the design targets are then tabulated and sorted in the form of Table 1.

If we choose to optimize over only the Schott glass catalog [47], then the number of different glasses available is $N = 110$. The algorithm provided in our code optimizes over any catalog, or any set of catalogs, provided with ZEMAX, but the Schott catalog is the one most widely used, and so is the one we choose here. After removing redundant and historical glasses, the Schott glass catalog is left with $N = 100$. The total number T_2 of unique glass pairs within this list is therefore $T_2 = N(N-1) = 9900$. (Because of nonlinearities in the design space, the ordering of the glasses *does* matter.) Although not all combinations are capable of satisfying both design targets simultaneously, the resulting table of designs produced by the algorithm is generally quite long, and so the list is then sorted by merit function value to show the best performing designs (see the authors' website [2] for example tables of designs). Assuming that the algorithm has successfully located the global minimum in the design space for each glass combination, the design whose merit function is lowest within the resulting list is the overall optimum for the given glass catalog (or set of catalogs).

Table 1. Best Performing Doublet Prisms for Design Targets $\bar{\delta}^* = 0$ and $\Delta^* = 1°$ ($400\,\text{nm} \le \lambda \le 700\,\text{nm}$, $\theta_0 = 0$)[a]

	Glass 1	Glass 2	α_1 (deg)	α_2 (deg)	$\bar{\delta}$ (deg)	Δ (deg)	NL ($\times 10^4$)	SSR
1a	N-PK51	N-BK10	−104.55	124.14	0.000	1.000	0.182	2.99
2a	N-BAF4	N-KZFS11	−114.72	104.49	0.000	1.000	0.193	2.71
3a	N-BAF52	N-KZFS4	−114.61	112.39	0.000	1.000	0.195	2.49
4a	N-KZFS4	N-BAF52	110.73	−112.78	0.000	1.000	0.205	2.53
5a	N-KZFS11	N-BAF4	99.32	−108.82	0.000	1.000	0.223	2.40
6a	N-LAK33A	N-BALF5	65.07	−103.62	−0.001	1.000	0.323	4.70
7a	N-LASF31A	N-BAF4	56.17	−91.94	0.000	1.000	0.324	5.22
8a	LAFN7	N-BASF2	82.49	−98.03	0.000	1.000	0.327	4.72
9a	N-LASF44	N-BAF10	76.74	−101.15	0.000	1.000	0.328	4.56
10a	N-LAF34	N-SSK5	79.81	−101.73	0.000	1.000	0.335	4.45
1b	N-SF66	N-LAK34	13.62	−17.36	0.000	1.000	0.742	11.25
2b	N-SF66	N-LAK33A	13.97	−17.21	0.000	1.000	0.748	11.34
3b	N-LAK34	N-SF66	−17.49	13.74	0.000	1.000	0.742	11.25
4b	N-LAK33A	N-SF66	−17.33	14.08	0.000	1.000	0.749	11.34
5b	N-SF66	N-LAK14	13.47	−17.98	0.000	1.000	0.740	11.24

[a]Rows 1a–10a list the designs in order of dispersion linearity (1a–5a are unconstrained, while 6a–10a are constrained to incidence angles <65°); 1b–5b list the designs ordered by thickness. Prisms 1a and 1b are illustrated in Fig. 7.

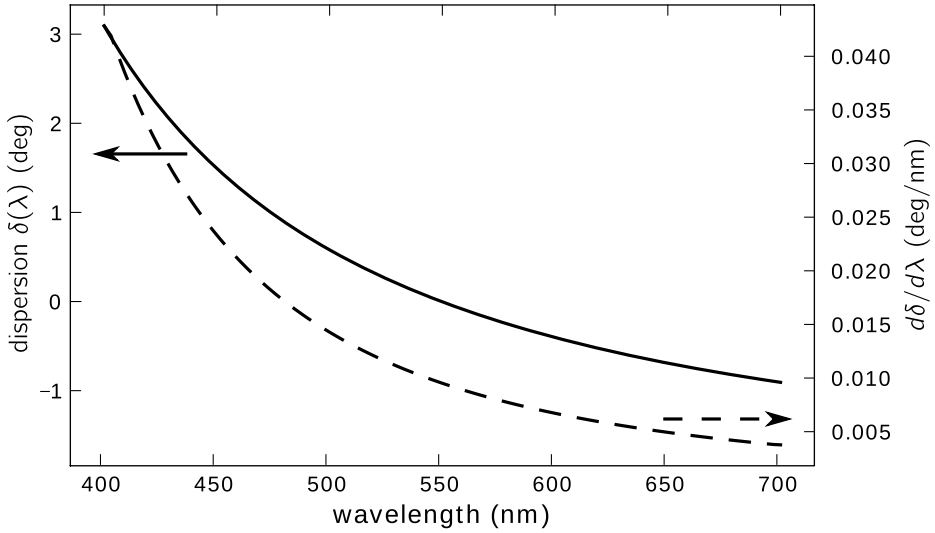

Fig. 6. Typical angular dispersion curve for a prism disperser (*left axis*) and the corresponding dispersion gradient (*right axis*). A detector array placed at the focal plane of a lens will provide a uniformly sampled spectrum if the dispersion gradient is constant across the spectrum. For the case shown here, the sampling will be 10× finer in the blue end of the spectrum than in the red.

6. Dispersion Linearity

Nonlinearity in the spectral dispersion (see Fig. 6) is often a nuisance to users of spectrometers, especially for spectrometers incorporating prism dispersing elements. We can attempt to minimize the dispersion nonlinearity (NL) by incorporating a penalty term into our design merit function. From Eq. (8), we know the ray deviation as a function of wavelength, $\delta(\lambda)$. The gradient of the deviation angle, $d\delta/d\lambda$, gives the spectral dispersion per unit wavelength. The difference of the gradient from a constant, or equivalently the area under the second derivative, gives a measure of the dispersion nonlinearity, defined as

$$\mathrm{NL} = \int \left|\frac{d^2\delta}{d\lambda^2}\right| \mathrm{d}\lambda. \tag{9}$$

Thus, the new merit function becomes

$$M = (\bar{\delta} - \bar{\delta}^*)^2 + (\Delta - \Delta^*)^2 + w_{\mathrm{nl}}\mathrm{NL}, \tag{10}$$

where w_{nl} is a weight factor for weighing the relative importance of the NL term versus the remaining terms of the merit function. In practice, the δ^* and Δ^* design constraints fix the values of α_1 and α_2 for a given glass choice, so that the first two terms of Eq. (10) become zero. In order to optimize for dispersion linearity, therefore, the only degree of freedom left is glass choice. Thus, the algorithm performs a brute force search over all glass combinations within the glass catalog in order to locate designs for which NL is smallest.

Another measure of the linearity of the spectrum is to take the ratio of the dispersion gradient maximum and minimum. This provides a measure of the maximum amount that the spectral bands get stretched by the nonlinear dispersion. This "spectral sampling ratio" (SSR) is defined as

$$\mathrm{SSR} = \max\left\{\left|\frac{d\delta}{d\lambda}\right|\right\} / \min\left\{\left|\frac{d\delta}{d\lambda}\right|\right\}. \tag{11}$$

Thus, for example, an SSR of 5 would mean that if the short wavelength end of the spectrum has a spectral bin that is 1 nm wide, the long wavelength end of the spectrum will have a spectral bin 5 nm wide.

Section (a) of Table 1 shows the best performing prisms from optimizing a $\bar{\delta}^* = 0$, $\Delta^* = 1°$ design over the Schott glass catalog. Only those prisms with the smallest NL are shown, with the first five designs (1a–5a) having angles of incidence unconstrained, and the second five (6a–10a) having angles of incidence constrained to <65°. We can see that in each case the two glasses chosen in Section (a) of the table tend to be close to one another on the Abbe diagram (i.e., they tend to have similar refractive indices $\bar{n}$ and similar linear dispersions V). (Note that the five glass combinations within each section of the table tend to be quite similar. The complete list of designs shows many different configurations, but these do not appear in the tables shown here due to space restrictions.)

Among the glass combinations in Table 1, we can see that the highly linear dispersion designs, which can have interface angles up to 89°, use a pair of glasses that lie very near one another on the glass chart, so that the glass–glass interface in the center of the prism induces very little beam deflection. When designing prisms for dispersion linearity, one finds that even for small amounts of dispersion (<1°), the angles of incidence on the prism interfaces can be substantial, indicating that these designs attempt to balance the dispersion equation's nonlinearity in incidence angle against the refractive index nonlinearity.

Constraining solutions to use angles of incidence less than a given value θ_{limit} (65° for the prisms of Table 1) can be accomplished by adding a

half-quadratic cost function to the merit function. For the I interfaces of a given prism ($I = 3$ for a doublet), we calculate

$$\Theta = \sum_{i=1}^{I} \begin{cases} 0, & \theta_i < \theta_{\text{limit}} \\ (\theta_{\text{limit}} - \theta_i)^2, & \theta_i > \theta_{\text{limit}} \end{cases}. \qquad (12)$$

Thus, the merit function is unaffected when a prism's interface angles remain under the limiting value, but increases quadratically as the design goes beyond θ_{limit}. The choice of 65° that we use here, rather than some other angle, is somewhat arbitrary, but has been selected as being small enough to be practical but large enough to allow sufficient design flexibility. Once we restrict the angles of the interface to <65°, we see the glass combinations in Table 1 change, so that now we have pairs of glasses with almost identical linear dispersion values (the Abbe V-number) but substantially different mean refractive indices.

One finds that, in general, direct-vision doublet prism designs have poorer dispersion linearity than their counterpart (non-direct-vision) singlet designs. Using the Schott glass catalog, the more linear singlet designs for $\Delta^* = 1°$ have $0.09 \le \text{NL} \le 0.12$, which lies below the doublet results shown in Table 1.

The bottom section of the Table 1 (designs 1b–5b) shows the thinnest designs. From this list, one can note that the best performing doublets use high-index glasses for both elements, and that among the high-index glasses, the linear dispersions of the two glasses chosen (i.e., V_1 and V_2) differ by as much as the catalog allows while keeping the mean refractive index relatively close. From the tabulated designs, one can note that the ordering of the glasses alters the performance somewhat. That is, if one flips the prism upside down and illuminates from the left instead of the right, the resulting dispersion is close to but not exactly the same as that of the original prism.

Note that direct-vision prisms with small dispersion values (<1°) are most commonly found in imaging spectrometry, where the number of spectral bands resolved is typically much smaller than in non-imaging spectrometry, and where the direct-vision geometry can provide substantial reduction in system size.

7. Doublet Prism Thickness

Another commonly desired characteristic is for a prism design to be as thin as possible. The overall prism thickness t can be defined by the sum of axial thicknesses as $t = t_1 + t_2$, or by taking the z distance from the prism extreme corners (i.e., front bottom edge to rear top edge, for the prism shown in Fig. 3). For an arbitrary prism height h, the former value can be obtained by the formulas

$$t_1 = h_0(\tan\gamma_1 - \tan\beta_1), \qquad t_2 = 2(h - h_0)\tan\beta_2,$$

where $h_0 = w\cos(\beta_1)/\cos(\theta_1)$. Here h_0 is the height from the optical axis to the first element apex and h is the full height of the element, from apex to base (see Fig. 3). All elements of the compound prism are assumed to share the same height h.

If an approximate relative measure of thickness t is all one needs, then one can also simply minimize the sum of apex angles, i.e., $t \approx h\sum_{i=1}^{I}|\alpha_1|$, in which h is the prism height and I the total number of prism elements. This approximate measure is what is used to sort the results shown in Table 1.

Taking a look at Fig. 7, we can see that for design 1a, the beam input is small relative to the prism height, indicating that for most systems this design will require large prisms. Here the prism height is three times that of the input beam width (i.e., $h \approx 3w$). This $h \gg w$ property is characteristic of all of the linearized designs 1a–5a in Table 1.

8. Achromatic Beam Deviation

So far, we have considered only direct-view dispersive prisms. One important prism application actually requires ray deviation without dispersion: beam steering [48]. With a small modification to our basic merit function, we can easily adopt the design algorithms to optimize for beam steering applications. While designing beam steering prisms, we run into the phenomenon of higher-order dispersion. Investigating this effect forces us once again to resort to asymmetric triplet prisms to achieve full performance.

Beam steering uses a set of rotating prism elements placed in front of an imaging system to steer the field of view within a much larger "field of regard" (see Fig. 8). In this application, dispersion in the deflected beam is unwanted, so it becomes necessary to achromatize with the proper selection of glasses and prism angles.

Although it is a well-known technique, published research on achromatic beam deviation is small enough to allow a nearly comprehensive citation list. The earliest publication of which we are aware is Ref. [33], an extremely scarce book available only in Russian. In the archive literature, one finds a handful of papers [49–55]. Only Ref. [52], however, presents a method for optimal glass selection, so that the reader is often left to wonder whether the results obtained are the best achievable. This is easily done, however, with the algorithms we have been working with so far.

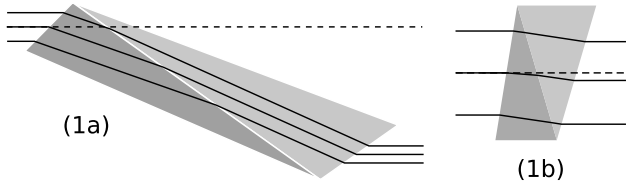

Fig. 7. Two prism designs from Table 1, design 1a (for improved dispersion linearity) and 1b (for a compact system). Both designs have $\bar{\delta}^* = 0$ and $\Delta^* = 1°$. The rays are drawn for the central wavelength, $\bar{\lambda}$. Note that both prisms show some negative beam displacement.

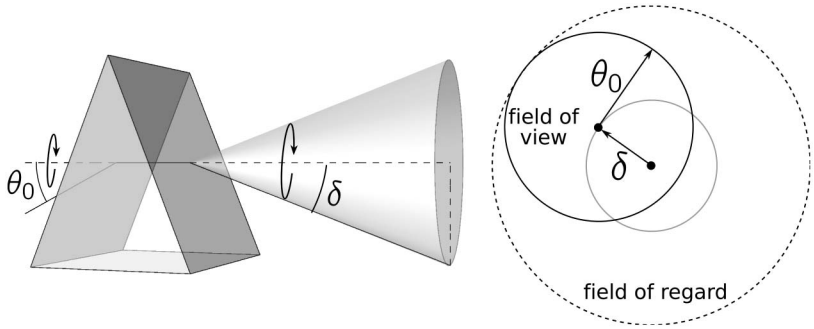

Fig. 8. As the prism is rotated, the deviation angle δ steers the field of view (with half-angle θ_0) through a wider "field of regard" (with half-angle $\delta + \theta_0$).

For achromatic beam deviation designs, we need only select a target central ray deviation $\bar{\delta}$ and dispersion value Δ (presumably zero in this case) as the inputs to our algorithm and run the code to provide a set of designs. However, for this application it is common to choose a slightly different form for the second term to limit the total change in deviation angle at all points across the spectral range. This leads to a new merit function

$$M_{\text{chr}} = (\bar{\delta} - \delta^*)^2 + C + \Theta, \tag{13}$$

where

$$C = |\max\{\delta(\lambda)\} - \min\{\delta(\lambda)\}|$$

is what we will call the "chromaticity." With this merit function, we optimize over all glass pair combinations within the catalog to obtain a design with minimum chromaticity.

Table 2 shows a list of doublet designs for achromatic 30° deviation across most of the visible spectrum, optimized across the Schott glass catalog (see Fig. 9 for chromaticity curves corresponding to designs 1b–5b). The results show that 30° deviation can be achieved with less than 20 mdeg of dispersion across the 450–650 nm spectral range. Note that the chromaticity generally decreases with higher angles of incidence θ_i allowed on the prism interfaces, so that the Θ term in Eq. (13) has a strong effect on the chromaticity.

The most compact designs in designs 1a–5a of Table 2 use a combination of the highest-dispersion glasses (SF68 and SF66) together with a glass that has one of the lowest ratios of partial dispersion to refractive index (LAK34, LAK14, LAK33A, and PSK53A).

9. Double Amici Prisms

The double Amici prism design is a three-element system (a "triplet") in which the first and third elements share the same glass and the same apex angles (see Fig. 10). The design layout is thus symmetric about the plane passing through the center of its second element. In general, if we allow air to be used as a "glass," then this layout can also model a pair of air-spaced singlet prisms. To allow this in our optimization code, we have added air as a glass to the standard catalog in each of our designs.

The symmetry property of the double Amici means that the linear design equations are almost identical to those of the doublet prism, with only the addition of a factor of 2 in front of the first term in each:

$$\bar{\delta} = 2\bar{\delta}_1 + \bar{\delta}_2 = 2(\bar{n}_1 - 1)\alpha_1 + (\bar{n}_2 - 1)\alpha_2,$$

$$\Delta = 2\frac{\bar{\delta}_1}{V_1} + \frac{\bar{\delta}_2}{V_2}.$$

Table 2. Achromatic Beam Deviation: the Best Performing Doublet Prisms (for $\theta_0 = 0$), Listed in Order of (a) Compactness or (b) Dispersion Chromaticity, Where Chromaticity C is Defined by Eq. (13)[a]

	Glass 1	Glass 2	α_1 (deg)	α_2 (deg)	$\bar{\delta}$ (deg)	C (×100)
		merit func.: M_{chr}, λ range = 450–650 nm, $\delta^* = 30°$, $\Delta^* = 0$				
1a	SF68	LAK34	−13.74	51.61	30.000	55.554
2a	SF68	LAK33A	−14.72	51.23	30.000	57.250
3a	SF68	PSK53A	−10.73	55.42	30.000	45.752
4a	SF68	LAK14	−13.24	53.08	30.000	55.694
5a	SF66	LAK34	−14.88	51.46	30.000	55.118
		merit func.: M_{chr}, λ range = 450–650 nm, $\delta^* = 30°$, $\Delta^* = 0$				
1b	SK5	CAF2	−39.89	93.20	30.000	0.210
2b	SK57	CAF2	−38.66	91.88	30.000	0.248
3b	SK11	CAF2	−41.70	92.76	30.000	0.251
4b	LAK21	CAF2	−35.14	92.39	30.000	0.253
5b	SK16	CAF2	−36.68	92.51	30.000	0.259

[a]The dispersions of prisms 1d–5d are illustrated in Fig. 9.

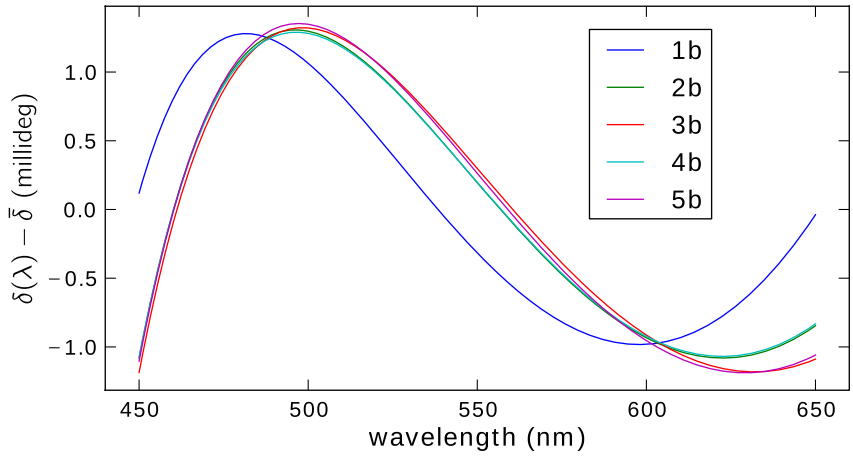

Fig. 9. (Color online) Dispersion, in millidegrees, of the achromatized beam deviation designs 1b–5b from Table 2.

Similar to Eq. (5), we can derive the expressions for the prism angles using the linear equations, giving

$$\alpha_1 = \frac{\Delta}{2(\bar{n}_1 - 1)}\left(\frac{1}{V_1} - \frac{1}{V_2}\right)^{-1},$$
$$\alpha_2 = \frac{\Delta}{\bar{n}_2 - 1}\left(\frac{1}{V_2} - \frac{1}{V_1}\right)^{-1}.$$

The nonlinear equation for the deviation angle δ requires including an additional two terms in the refraction equations, so that

$$\left.\begin{aligned}
&\theta_1 = \theta_0 - \beta_1, && \theta_3' = \arcsin\left(\tfrac{n_2}{n_1}\sin\theta_3\right),\\
&\theta_1' = \arcsin\left(\tfrac{1}{n_1}\sin\theta_1\right), && \theta_4 = \theta_3' - \alpha_1,\\
&\theta_2 = \theta_1' - \alpha_1, && \theta_4' = \arcsin(n_1\sin\theta_4),\\
&\theta_2' = \arcsin\left(\tfrac{n_1}{n_2}\sin\theta_2\right), && \theta_5 = \theta_4' - \beta_1\\
&\theta_3 = \theta_2' - \alpha_2,
\end{aligned}\right\} \quad (14)$$

can be concatenated to form $\delta(n_1(\lambda), n_2(\lambda), \alpha_1, \alpha_2, \theta_0)$. Here $\beta_1 = -\alpha_1 + \frac{1}{2}\alpha_2$ and $\delta = \theta_0 - \theta_5$.

Figure 11 shows the (α_1, α_2) design space for a fused silica/N-LASF31A/fused silica double Amici prism used in the 400–700 nm spectral range. We can see that the design space for the central deviation is still well behaved, and that the design space for the dispersion has begun to diverge significantly from linearity. And we also find that for the design targets of $\bar{\delta}^* = 0$ and $\Delta^* = 2°$, the linear equations provide a design $(\alpha_1, \alpha_2) = (95.4°, -98.6°)$, which lies *outside* the valid design space, where total internal reflection occurs at an interface between one of the prism elements. The nonlinear algorithm indicates an optimum solution located at $(\alpha_1, \alpha_2) = (64.9°, -63.6°)$. Additionally, the minimum for $|\Delta - \Delta^*|$ occurring in the bottom right corner of the design space has deepened, making it easier for an optimization algorithm to get trapped there.

Note that the double Amici prism, despite having an element more than the doublet, does not actually have additional degrees of freedom for design. Thus, after achieving the design targets $\bar{\delta}^*$ and Δ^*, the only means of optimizing auxiliary design variables such as dispersion linearity or total thickness is to adjust the glass types. Accordingly, as with the doublet design, we perform a complete search over all glass pairs available within the glass catalog.

Table 3 shows the best designs resulting from our algorithm, as determined by either dispersion linearity or system thinness. Because the "achromatizing" effect of the glasses in a double Amici prism is less severe than in a simple direct-vision doublet, we find

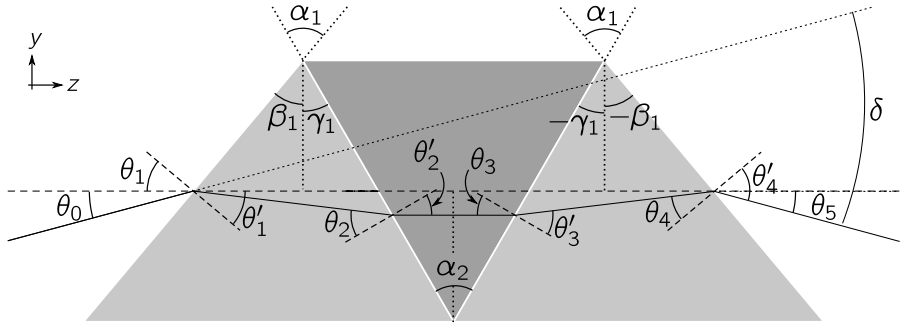

Fig. 10. Raytrace through a double Amici prism: the first and third elements are identical, and the second element is oriented symmetrically with respect to the normal to the optical axis. The system shown here has prism apex angles $\alpha_1 = 70°$ and $\alpha_2 = -60°$, indices of refraction $n_1 = 1.5$ and $n_2 = 1.8$, height h, and axial thicknesses t_1 and t_2. The input ray has angle $\theta_0 = 15°$, such that $\delta = 30°$. For this setup, the beam displacement Δy is nearly zero.

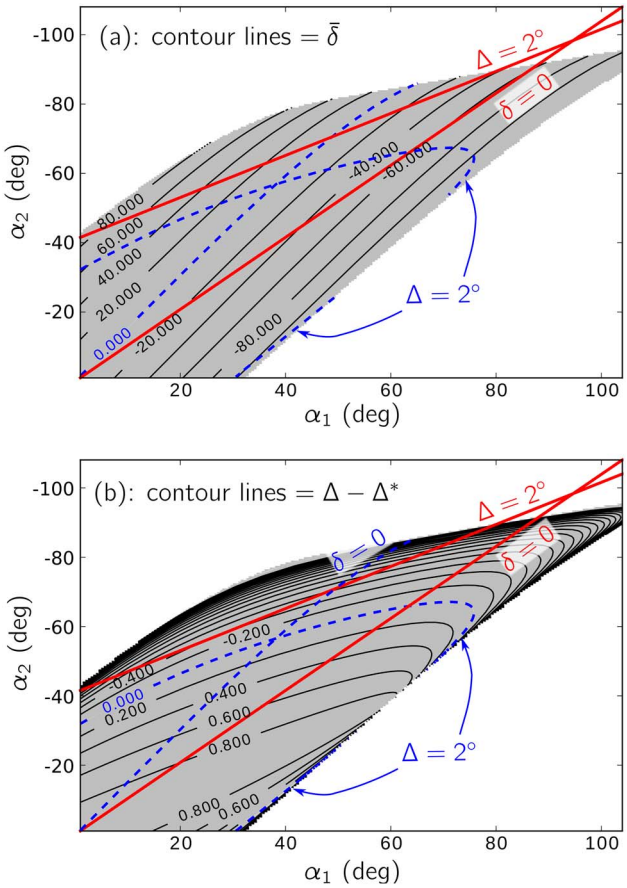

Fig. 11. (Color online) Double Amici prism design space, showing contour plots of (a) the deviation δ and (b) the dispersion Δ for a 400–700 nm spectral range, and for a fused silica/N-LASF31A/fused silica glass triplet, with (a) $\bar{\delta}^* = 0$ and (b) $\Delta^* = 2°$. As in Fig. 4, the dashed blue line indicates (α_1, α_2) designs meeting target values, the red solid lines indicate designs using linear Eq. (5), and the gray background indicates the valid design space.

that substantially greater dispersion is possible. Comparing the designs in Tables 1 and 3, we find that the double Amici designs can achieve much larger dispersion (23.5° instead of 14° in the case of design 1b in Table 1 versus design 1c in Table 3). Dispersion of 23.5° across the visible spectrum (400–700 nm) is roughly equivalent to that of a 1300 lines/mm diffraction grating, while still achieving direct-view geometry (zero mean beam deviation). The double Amici design angles as a function of dispersion are illustrated in Fig. 12 for N-LAK34 and N-SF66 glasses. Note that the doublet and double Amici designs of Figs. 5 and 12 use the same glasses and the same spectral range. If we restrict the prism design space to systems having maximum angles of incidence of 65°, then we obtain the designs shown.

Comparing the double Amici prisms of Table 1's section (a) with their doublet counterparts, we can see a modest improvement in the linearity, and very similar glass combinations. Comparing the prisms with the most linear dispersion (in Table 1 section (b)) with the most compact designs (Table 1 section (c)), we find that there is not a lot of flexibility in this design space. If we allow angles of incidence >65°, then the linearity can improve dramatically, but the cost is a prism that is quite large in comparison to the transmitted beam size. At smaller amounts of dispersion, the trade-off is less severe, and substantial improvements in dispersion linearity can be achieved.

The double Amici glass choices in Table 3 differ from the doublets of Table 1 in glass composition: the highly linear double Amici designs use a very low dispersion glass combined with an LAK/LAF glass, while the thinnest designs use a pair of highly dispersive materials. Figure 13 illustrates the layouts and dispersions for prism designs 1b and 1c from Table 3,

Table 3. Best Performing Double Amici Prisms for Design Targets $\bar{\delta}^* = 0$ and $\Delta^* = 4°$ ($400\,\text{nm} \le \lambda \le 700\,\text{nm}$, $\theta_0 = 0$)[a]

	Glass 1	Glass 2	α_1 (deg)	α_2 (deg)	$\bar{\delta}$ (deg)	Δ (deg)	NL ($\times 10^4$)	SSR
			λ range: 400–700 nm, $\Delta^* = 1°$, sorted by linearity					
1a	N-BAF4	P-LASF47	−82.04	106.98	0.006	0.903	0.239	4.31
2a	N-BAF4	N-LASF31A	−81.86	97.68	0.000	1.000	0.269	4.54
3a	N-BAF52	N-LASF41	−82.24	103.91	0.000	1.000	0.302	4.79
4a	N-BALF5	N-LAF34	−85.66	104.26	0.002	0.929	0.336	5.55
5a	LITH-CAF2	N-FK5	−74.33	121.63	0.002	0.951	0.339	4.04
			λ range: 400–700 nm, $\Delta^* = 4°$, sorted by linearity					
1b	LITH-CAF2	N-LAK33A	−95.04	94.37	0.000	4.000	1.770	5.74
2b	LITH-CAF2	N-LAF34	−92.05	90.50	0.000	4.000	1.814	5.97
3b	LITH-CAF2	N-LAF35	−92.08	93.38	0.000	4.000	1.830	6.03
4b	LITH-CAF2	N-LAF21	−89.48	87.24	0.001	4.000	1.859	6.13
5b	LITH-CAF2	N-LASF44	−88.17	84.87	0.000	4.000	1.860	6.21
			λ range: 400–700 nm, $\Delta^* = 4°$, sorted by thickness					
1c	N-LAK34	N-SF66	−32.57	50.29	0.000	4.000	2.995	11.35
2c	N-SF66	N-LAK34	25.09	−65.70	0.000	4.000	2.937	11.09
3c	N-LAK33A	N-SF66	−32.23	51.55	0.000	4.000	3.019	11.45
4c	N-SF66	N-LAK33A	25.77	−64.97	0.000	4.000	2.962	11.18
5c	N-LAK14	N-SF66	−33.68	49.57	0.000	4.000	2.984	11.33

[a]Sections (a) and (b) of the table list the designs in order of dispersion linearity; section (c) lists the designs ordered by thickness. All of the designs are constrained to angles of incidence <65°. The layout and dispersions for prisms 1a and 1b are illustrated in Fig. 13.

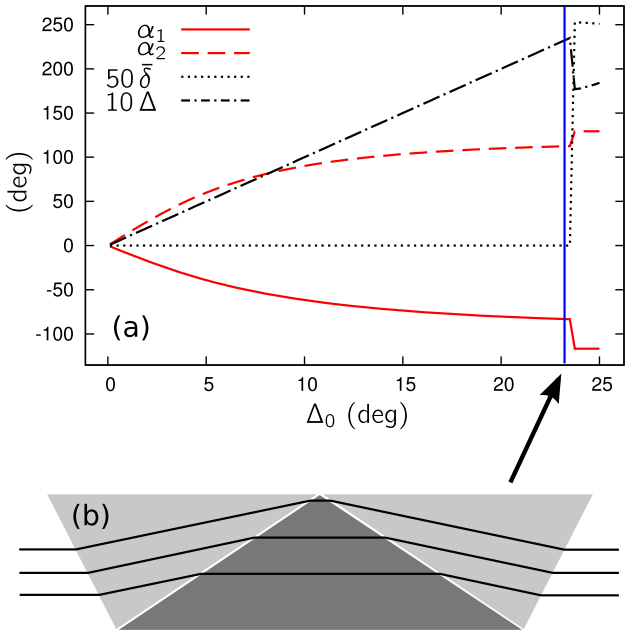

Fig. 12. (Color online) (a) Design parameters of a nondeviating N-LAK34/N-SF66 double Amici prism as a function of the target dispersion. The kink in the curves occurs at $\Delta^* = 23.5°$, beyond which the system can no longer achieve the target values. The vertical bar at the right side of the plot indicates the design configuration whose layout is shown in (b).

showing again that trying to achieve dispersion linearity involves a trade-off in prism compactness. For prisms with more modest amounts of dispersion (<1° for dispersion across the full visible spectral range, for example), the linearity achievable is greatly increased. Thus, the fact that sections (b) and (c) of Table 3 have similar values of NL (within a factor of 2) is a result of the confined design space available for 4° dispersion across this spectral range.

Among the designs shown in Table 3, we can see that the dispersion linearity is substantially worse than for the doublet designs—a result due entirely to the higher spectral dispersion requirements in the double Amici designs. If we compare double Amici prisms with doublets having the *same* dispersion, however, we find what one would intuitively expect: a double Amici's dispersion designs can be made more linear than an equivalent doublet's can.

One feature that a double Amici design can achieve that is difficult to accomplish with a doublet is zero beam displacement (i.e., $\Delta y = 0$). In some optical systems, and especially in prism arrays, it may be problematic to allow substantial beam displacement, and this can be an important design constraint. This $\Delta y = 0$ bound creates a nonlinear constraint on the relationship between θ_0, α_1, α_2, $\bar{n}_1$, and $\bar{n}_2$. Also, since the beam deviation is a function of wavelength, the beam displacement Δy will vary across the spectrum, so that zero displacement is typically achieved for only one wavelength and only one angle of incidence. In typical double Amici prisms, however, the chromatic transverse displacement is quite small for on-axis illumination ($\theta_0 = 0$).

If we assume $\theta_0 = 0$, then zero displacement will occur when the ray inside the second element is parallel to the optical axis (i.e., $\theta_2' = -\beta_2$). This simplifies the equation of constraint (for $\Delta y = 0$) relating α_1 and α_2 to

$$\frac{\alpha_2}{2} = \arcsin\left(\frac{\bar{n}_1}{\bar{n}_2}\sin\left(\alpha_1 + \arcsin\left(\frac{1}{\bar{n}_1}\sin\beta_1\right)\right)\right).$$

Under the small-angle approximations, this can be further approximated by the simple linear equation

$$\bar{n}_2 = 2\bar{n}_1 - 1.$$

Thus, in order to achieve zero beam displacement, we can expect the interior element of a double Amici prism to use very high-index glasses, and the exterior elements to use very low-index glasses, in order to satisfy this constraint. Calcium fluoride (i.e., LITHOTEC-CAF2, $\bar{n} = 1.436$) and N-LAK33A ($\bar{n} = 1.762$)—two prominent glasses in Table 3—do not

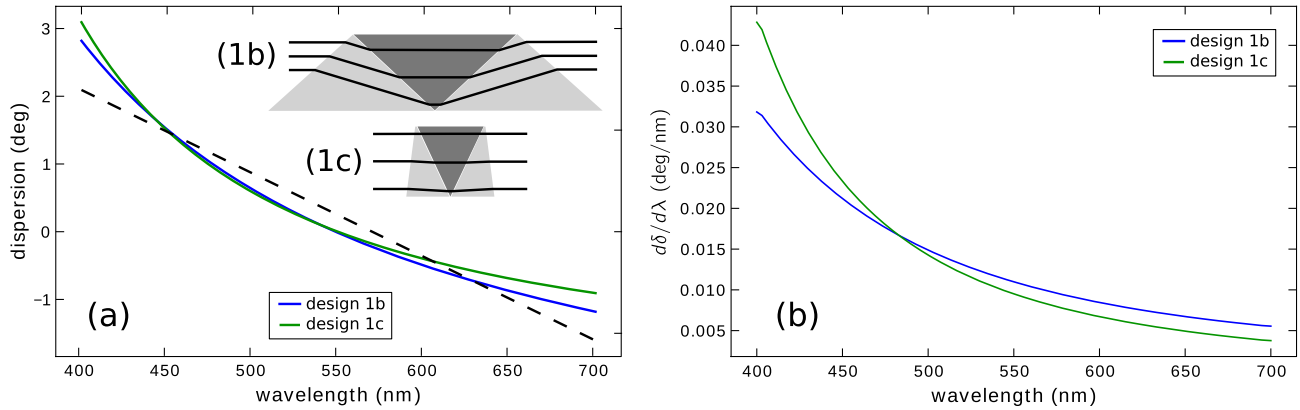

Fig. 13. (Color online) Layout, dispersion, and dispersion gradient for prism designs 1b and 1c from Table 3. The rays drawn in the prism layouts are for the central wavelength, $\bar{\lambda}$. The dashed line in (a) is the best-fit linear portion of 1b's dispersion curve. The gradient curves in (b) indicate that the spectral sampling rate in the blue end of the spectrum will be 6× (design 1b) or 10× (design 1c) that in the red end due to dispersion NL.

quite satisfy this relation, and so allow some beam displacement. A glass pair that gives very low displacement is fused silica (i.e., LITHOSIL-Q, $\bar{n} = 1.462$) and P-SF67 ($\bar{n} = 1.933$).

10. Conclusion

Historically, the first spectrometers used prisms as dispersing elements, a characteristic that continued until the development of advanced ruling engines and high-resolution grating spectrometers in the twentieth century. With these new grating dispersers, the use of prisms declined sharply, a trend driven in part by problems with volume absorption within the prism glass and the lack of good antireflection coatings on the prism interfaces. Gratings acquired a reputation not only of having much stronger dispersion, but also of having greater throughput. But the modern development of high-purity glasses and excellent thin film coatings has largely eliminated prisms' difficulties with absorption and partial reflections. In contrast, gratings still struggle with the loss and stray light incurred due to light diffracted into unwanted diffraction orders. For the modern optical designer, prisms can thus provide higher throughput as well as decreased stray light.

There remains a strong perception among designers that prisms are incapable of providing dispersion comparable to gratings. The results of Section 9, however, show that with a proper choice of glasses, compound prisms can provide comparable dispersion to that of many gratings, even while maintaining a direct-vision geometry. There also remains a perception, derived from well-known theory [56] that prisms will always have a lower resolving power than their grating counterparts, a result based on the assumption of using singlet prisms in their minimum deviation geometry. We have shown, however, that compound prisms can achieve substantially higher dispersion than singlets can, while also maintaining the input beam width, such that the resolving power will actually surpass that of gratings with equivalent dispersion.

Finally, compound prisms provide a number of degrees of freedom with which to customize the dispersion characteristics, allowing one to tune the disperser to any special system requirements. This is a flexibility that is largely unavailable to standard gratings, though it can be realized by combining gratings with singlet prisms [57]. Thus, while high-quality compound prisms may be more expensive than comparable gratings, their throughput is often much higher, their design flexibility is greater, and their direct-vision capability can be a substantial advantage when system compactness is needed.

In order to take advantage of these features, however, an optical designer needs to have a better understanding of the design space than that provided by the conventional linear design as in Eqs. (2)–(7). Commercial optical design software provides all of the necessary functionality for this work, but can be clumsy to customize for the special requirements of compound prism design. For example, although the prism apex angle α design parameter is a continuous variable, and thus easy for optimization routines to use, the glass refractive index and dispersion $n(\lambda)$ is a discrete quantity constrained by available glass choices. Optimizing over glasses thus requires a search over available glass combinations. And due to the nonlinear design space, tailoring the merit function is a necessity for obtaining a good set of designs from which to choose.

In the third paper of this series [18], we go on to use the methods described here to design linear-in-wavenumber prisms, a property that turns out to be much easier to achieve than linearity in wavelength. Dispersion linearity in wavenumber allows us to design high-dispersion direct-vision prisms specifically for the demanding application of optical coherence tomography, which also requires using alternative glasses for the near-infrared spectral range.

Among the designs shown in Sections 4 and 9 above, one of the undesirable properties of prism spectra is their dispersion nonlinearity. Although one can select the optimal glass combination, this has limited ability to improve on the dispersion linearity. In order to achieve a large improvement in linearity, it is necessary to add more degrees of freedom into the design, such as using asymmetric three-element prisms ("triplets") or symmetric five-element prisms (Janssen prisms). These compound prisms have sufficient degrees of freedom to provide impressive performance, in both dispersion linearity and dispersive power, while maintaining direct-view geometry.

We encourage interested readers to download and modify the design code we have written for this work, available at the authors' website [2].

This work was partially supported by National Institutes of Health (NIH) grants RO1-CA124319 and R21-EB009186.

References and Note

1. G. B. Donati, "Intorno alle strie degli spettri stellari [On lines in stellar spectra]," Annali del Reale Museo di Fisica e Storia Naturale di Firenze **1**, 1–20 (1866), in Italian.
2. http://www.owlnet.rice.edu/~tt3/.
3. G. B. Donati, "Intorno alle strie degli spettri stellari [On lines in stellar spectra]," Nuovo Cimento **15**, 292–304 (1862), in Italian.
4. G. B. Donati, "Memorie astronomiche," Mon. Not. R. Astron. Soc. **23**, 100–107 (1863).
5. P. J. C. Janssen, "Note sur trois spectroscopes [Note on three spectroscopes]," C.R. Hebd. Seances Acad. Sci. **55**, 576–578 (1862), in French.
6. J. N. Lockyer, *The Spectroscope and its Applications* (Macmillan, 1873).
7. P. A. Secchi, *Le Stelle [The Stars]* (Dumolard, 1877), in Italian.
8. J. P. Gassiot, "Description of a train of eleven sulphide-of-carbon prisms arranged for spectrum analysis," Proc. R. Soc. London **13**, 183–185 (1864).
9. J. Browning, "Note on the use of compound prisms," Mon. Not. R. Astron. Soc. **31**, 203–205 (1871).
10. A. S. Herschel, "Direct vision spectroscopes by double internal reflection," Intellectual Observer **7**, 444–447 (1865).

11. H. Schellen, *Spectrum Analysis in its Application to Terrestrial Substances and the Physical Constitution of the Heavenly Bodies* (Appleton, 1872), p.82, translated by J. Lassell and C. Lassell.
12. H. Emsmann, "Ein spectroskop à vision directe mit nur einem prisma [A direct vision spectroscope with a single prism]," Ann. Phys. **150**, 636–640 (1873), in German.
13. F. Fuchs, "Vorschläge zur construction einiger optischer vorichtungen [Proposals for construction of some optical devices]," Z. Instrumentenkd. **1**, 326–329 (1881), in German.
14. G. D. Liveing and J. Dewar, "Note on a new form of direct vision spectroscope," Proc. R. Soc. London **41**, 449–452 (1886).
15. M. V. R. K. Murty and A. L. Narasimham, "Some new direct vision dispersion prism systems," Appl. Opt. **9**, 859–862 (1970).
16. P. G. Tait, "On anomalous spectra, and on a simple direct-vision spectroscope," Proc. R. Soc. Edinburgh **7**, 410–414 (1872).
17. N. Hagen and T. S. Tkaczyk, "Compound prism design principles, II: triplet and Janssen prisms," Appl. Opt. **50**, 5012–5022 (2011).
18. N. Hagen and T. S. Tkaczyk, "Compound prism design principles, III: linear-in-wavenumber and OCT prisms," Appl. Opt. **50**, 5023–5030 (2011).
19. A. Thollon, "Nouveau spectroscope [A new spectroscope]," J. Phys. Theor. Appl. **7**, 141–148 (1878), in French.
20. A. Thollon, "Théorie du nouveau spectroscope à vision directe [Theory of the new direct vision spectroscope]," C.R. Hebd. Seances Acad. Sci. **86**, 595–598 (1878), in French.
21. A. Riccó, "Combinazioni spettroscopiche a visione diretta [Combinations for direct vision spectroscopy]," Mem. Soc. Astron. Ital. **8**, 21–34 (1879), in Italian.
22. A. Thollon, "Spectroscopes à vision directe et a grande dispersion [Direct vision spectroscopes with large dispersion]," J. Phys. Theor. Appl. **8**, 73–77 (1879), in French.
23. K. W. Zenger, "Ueber ein neues spectroskop mit gerader durchsicht [On a new direct view spectroscope]," Z. Instrumentenkd. **1**, 263–266 (1881), in German.
24. W. Wernicke, "Neues Flüssigkeitsprisma für Spectralapparate [A new liquid prism for spectroscopes]," Z.Instrumentenkd. **1**, 353–357 (1881), in German.
25. H. J. V. Tyrrell and G. K. T. Conn, "The optical properties of a compound liquid prism suitable for studies of the Raman effect," J. Opt. Soc. Am. **42**, 106–113 (1952).
26. C. G. Abbott, J. Fowle, and E. Frederick, "A prism of uniform dispersion," Astrophys. J. **11**, 135–139 (1900).
27. N. Ebizuka, H. Yokota, F. Kajino, K. S. Kawabata, M. Iye, and S. Sato, "Novel direct vision prism and Wollaston prism assembly for diffraction limit applications," Proc. SPIE **7018**, 70184S (2008).
28. F. Blechinger, B. Harnisch, and B. Kunkel, "Optical concepts for high resolution imaging spectrometers," Proc. SPIE **2480**, 165–179 (1995).
29. R. Bittner, Y. Delclaud, G. Cerutti-Maori, and J.-Y. Labandibar, "Spectra apparatus of the concentric type having a Fery prism," U. S. patent 5,781,290 (14 July 1998).
30. M. Herzberger and N. R. McClure, "The design of superachromatic lenses," Appl. Opt. **2**, 553–560 (1963).
31. R. E. Stephens, "Selection of glasses for three-color achromats," J. Opt. Soc. Am. **49**, 398–401 (1959).
32. E. L. Dereniak and T. D. Dereniak, *Geometric and Trigonometric Optics* (Cambridge University, 2008), pp.347–350.
33. V. N. Churilovskii, *Raschet Prizmennykh System [The Design of Prism Systems]* (Leningrad, 1933), in Russian.
34. C. G. Wynne, "Atmospheric dispersion in very large telescopes with adaptive optics," Mon. Not. R. Astron. Soc. **285**, 130–134 (1997).
35. A. A. Wagadarikar, N. P. Pitsianis, X. Sun, and D. J. Brady, "Video rate spectral imaging using a coded aperture snapshot spectral imager," Opt. Express **17**, 6368–6388 (2009).
36. R. T. Kester, L. Gao, and T. S. Tkaczyk, "Development of image mappers for hyperspectral biomedical imaging applications," Appl. Opt. **49**, 1886–1899 (2010).
37. J. E. Greivenkamp, *Field Guide to Geometrical Optics* (SPIE, 2004), p. 1.
38. R. D. Stigler, "Non-deviating prism with continuously variable dispersion," U. S. patent 5,610,771 (11 March 1997).
39. A. K. Brodzik and J. M. Mooney, "Convex projections algorithm for restoration of limited-angle chromotomographic images," J. Opt. Soc. Am. A **16**, 246–257 (1999).
40. D. A. LeMaster, "Design and model verification of an infrared chromotomographic imaging system," Master's thesis (Air Force Institute of Technology, 2004).
41. J. M. Mooney, W. S. Ewing, and R. J. Nelson, "Multi-band direct vision prism," U. S. patent 6,935,757 (30 August 2005).
42. R. W. Deming, "Chromotomography for a rotating-prism instrument using backprojection, then filtering," Opt. Lett. **31**, 2281–2283 (2006).
43. The actual optimization algorithm used in our design code is SciPy's `fmin` function, which uses a Nelder–Mead simplex algorithm. Many other algorithms were tested and work equally well, with `fmin` being the fastest among them.
44. S. E. Holland, D. E. Groom, N. P. Palaio, R. J. Stover, and M. Wei, "Fully depleted, back-illuminated charge-coupled devices fabricated on high-resistivity silicon," IEEE Trans. Electron Devices **50**, 225–238 (2003).
45. S. E. Holland, W. F. Kolbe, and C. J. Bebek, "Device design for a 12.3-megapixel, fully depleted, back-illuminated, high-voltage compatible charge-coupled device," IEEE Trans. Electron Devices **56**, 2612–2622 (2009).
46. ZEMAX Development Corp., www.zemax.com.
47. http://www.us.schott.com/advanced_optics/english/our_products/materials/data_tools/.
48. W. Smith, *Modern Optical Engineering*, 4th ed. (McGraw-Hill Professional, 2007), pp.126–128.
49. E. N. Goncharenko and G. N. Repinskii, "The design of achromatic wedges," Sov. J. Opt. Technol. **42**, 445–448 (1975).
50. N. V. Sheinis, "Design of a wedge scanner," Sov. J. Opt. Technol. **43**, 473 (1976).
51. J. Lacoursière, M. Doucet, E. Curatu, M. Savard, S. Verreault, S. Thibault, P. Chevrette, and B. Ricard, "Large-deviation achromatic Risley prisms pointing systems," Proc. SPIE **4773**, 123–131 (2002).
52. B. D. Duncan, P. J. Bos, and V. Sergan, "Wide-angle achromatic prism beam steering for infrared countermeasure applications," Opt. Eng. **42**, 1038–1047 (2003).
53. K. Kim, D. Kim, K. Matsumiya, E. Kobayashi, and T. Dohi, "Wide FOV wedge prism endoscope," Proc. Annu. Conf. Eng. Med. Biol. **6**, 5758–5761 (2005).
54. P. J. Bos, H. Garcia, and V. Sergan, "Wide-angle achromatic prism beam steering for infrared countermeasures and imaging applications: solving the singularity problem in the two-prism design," Opt. Eng. **46**, 113001 (2007).
55. Y.-J. Lin, K.-M. Chen, and S.-T. Wu, "Broadband and polarization-independent beam steering using dielectrophoresis-tilted prism," Opt. Express **17**, 8651–8656 (2009).
56. M. Born and E. Wolf, *Principles of Optics*, 7th ed. (Cambridge University, 1999), pp. 452–453.
57. Z. Hu and A. M. Rollins, "Fourier domain optical coherence tomography with a linear-in-wavenumber spectrometer," Opt. Lett. **32**, 3525–3527 (2007).